

A New Generalized Chaplygin Gas as a Scheme for Unification of Dark Energy and Dark Matter

Xin Zhang^{1,2}, Feng-Quan Wu^{1,2}, and Jingfei Zhang³

1 CCAST (World Laboratory), P.O.Box 8730, Beijing 100080, People's Republic of China

2 Institute of High Energy Physics, Chinese Academy of Sciences, P.O.Box 918(4), Beijing 100049, People's Republic of China

3 Department of Physics, Liaoning Normal University, Dalian 116029, People's Republic of China

Abstract

We propose in this paper a new model for describing the unification of dark energy and dark matter. This new model is a further generalization of the generalized Chaplygin gas (GCG) model, thus dubbed new generalized Chaplygin gas (NGCG) model. The equation of state of the NGCG is given by $p = -\tilde{A}(a)/\rho^\alpha$, where a is the scale factor and $\tilde{A}(a) = -w_X A a^{-3(1+w_X)(1+\alpha)}$. We show that the NGCG model is totally dual to an interacting XCDM parametrization scenario, in which the interaction between dark energy and dark matter is characterized by the constant α . We discuss the cosmological consequences led by such an unified dark sectors model. Furthermore, we perform a statefinder analysis on this scenario and show the discrimination between this scenario and other dark energy models. Finally, a combined analysis of the data of Type Ia supernovae, cosmic microwave background, and large scale structure provides a fairly tight constraint on the parameters of the NGCG model.

I. INTRODUCTION

Recent observations of Type Ia supernovae (SNe Ia) [1] indicate that the expansion of the Universe is accelerating at the present time. These results, when combined with the observations of cosmic microwave background (CMB) [2] and large scale structure (LSS) [3], strongly suggest that the Universe is spatially flat and dominated by an exotic component with large negative pressure, referred to as dark energy [4]. The first year result of the Wilkinson Microwave Anisotropy Probe (WMAP) shows that dark energy occupies about 73% of the energy of our Universe, and dark matter about 23%. The usual baryon matter which can be described by our known particle theory occupies only about 4% of the total energy of the Universe. Although we can affirm that the ultimate fate of the Universe is determined by the feature of dark energy, the nature of dark energy as well as its cosmological origin remain enigmatic at present. So far the confirmed information about dark energy is still limited and can be roughly summarized as the following several items: it is a kind of exotic energy form with sufficiently large negative pressure such that drives the Universe to undergo a period of accelerating expansion currently; it is spatially homogeneous and non-clustering; and it is in small part at the early times while dominates the Universe very recently.

The investigation of the nature of dark energy is an important mission in the modern cosmology. Much work has been done on this issue, and there is still a long way to go. Currently, the preferred candidates of dark energy are vacuum energy (or cosmological constant) and dynamical fields. The simplest form of dark energy is the cosmological constant Λ . A tiny positive cosmological constant which can naturally explain the current acceleration would encounter many theoretical problems, such as the “fine-tuning” problem and the “coincidence” problem. Another possible form of dark energy is provided by scalar fields. Dark energy can be attributed to the dynamics of a scalar field ϕ , called quintessence [5], which convincingly realize the present accelerated expansion of the Universe by evolving slowly down its potential $V(\phi)$. The tracker version quintessence is to some extent likely to resolve the coincidence problem. It should also be pointed out that the coupled quintessence models [6] provide this problem with a more natural solution. However, for quintessence models with flat potentials, the quintessence field has to be nearly massless and one thus expects radiative corrections to destabilize the ratio between this mass and the other known scales of physics. In addition, for the cosmological constant and many quintessence models, the event horizon would lead to a potential incompatibility with the string theory.

Other designs on dark energy roughly include k-essence [7], quiescence (or “X-matter”) [8], brane world [9], tachyon [10], generalized Chaplygin gas (GCG) [11,12], holographic dark energy [13,14], and so forth. The quiescence or X-matter component is simply characterized

by a constant, non-positive equation of state w_X ($w_X < -1/3$ is a necessary condition to make the Universe accelerate). In general, in a Friedmann-Robertson-Walker (FRW) background with the presence of cold dark matter (CDM), an arbitrary but constant w_X for dark energy from the range $(-1, 0)$ can be achieved by using a scalar field with a hyperbolic sine potential [8]. It may be noted that in principle the value of w_X may be even less than -1 . In fact, by fitting the SNe Ia data in the framework of XCDM (X-matter with CDM), the hint for $w_X < -1$ has been found. Indeed, a study of high- z SNe Ia [15] finds that the equation of state of dark energy has a 99% probability of being < -1 if no priors are placed on Ω_m^0 . When these SNe results are combined with CMB and 2dFGRS the 95% confidence limits on an unevolving equation of state are $-1.46 < w_X < -0.78$ [15,16] which is consistent with estimates made by other groups [2,3]. The possibility of $w_X < -1$ has provoked lots of investigations on the phantom dark energy [17]. The remarkable feature of the phantom model is that the Universe will end its life with a “Big Rip” (future singularity) within a finite time [18]. On the other hand, we concern here another interesting proposal on dark energy, i.e. the dark energy component might be explained by a background fluid with an exotic equation of state, the generalized Chaplygin gas model [11]. The striking feature of this model is that it allows for a unification of dark energy and dark matter. This point can be easily seen from the fact that the GCG behaves as a dust-like matter at early times and behaves like a cosmological constant at late stage. This dual role is at the heart of the surprising properties of the GCG model. Moreover, the GCG model has been successfully confronted with various phenomenological tests involving SNe Ia data, CMB peak locations, gravitational lensing and other observational data [12]. It is remarkable that the GCG equation of state has a well defined connection with string and brane theories [19], and this gas is the only gas known to admit a supersymmetric generalization [20].

In addition, it should be pointed out that the GCG model can be portrayed as a picture that cosmological constant type dark energy interacts with cold dark matter. However, since the equation of state of dark energy still cannot be determined exactly, the observational data show w_X is in the range of $(-1.46, -0.78)$, the GCG model should naturally be generalized to accommodate any possible X-type dark energy with constant w_X . Therefore, we propose here a new generalized Chaplygin gas (NGCG) scenario as a scheme for unification of X-type dark energy and dark matter. The feature of this new model should also be exhibited in that dark sectors are uniformly described by an exotic background fluid and this new gas behaves as a dust-like matter at early times and as a X-type dark energy at late times. We will show in this paper that this model is a kind of interacting XCDM model, and constrain the parameters of this model by using observational data.

This paper is organized as follows. In Section 2, we introduce the extension version of

the generalized Chaplygin gas, namely the NGCG model, to describe the unification of dark energy and dark matter, and demonstrate that the NGCG actually is a kind of interacting Λ CDM system. In Section 3, we analyze the NGCG model by means of the statefinder parameters. In Section 4, we constrain the parameters of the NGCG model using the SNe Ia, CMB, and LSS data. We give concluding remarks in the final section.

II. THE NGCG SCENARIO AND THE INTERACTING Λ CDM PARAMETRIZATION

In this section we introduce the NGCG model. In the framework of FRW cosmology, considering an exotic background fluid, the NGCG, described by the equation of state

$$p_{\text{Ch}} = -\frac{\tilde{A}(a)}{\rho_{\text{Ch}}^\alpha}, \quad (1)$$

where α is a real number and $\tilde{A}(a)$ is a function depends upon the scale factor of the Universe, a . We might expect that this exotic background fluid smoothly interpolates between a dust dominated phase $\rho \sim a^{-3}$ and a dark energy dominated phase $\rho \sim a^{-3(1+w_X)}$ where w_X is a constant and should be taken as any possible value in the range $(-1.46, -0.78)$. It can be expected that the energy density of the NGCG should be elegantly expressed as

$$\rho_{\text{Ch}} = \left[Aa^{-3(1+w_X)(1+\alpha)} + Ba^{-3(1+\alpha)} \right]^{\frac{1}{1+\alpha}}. \quad (2)$$

The derivation of the Eq. (2) should be the consequence of substituting the equation of state Eq. (1) into the energy conservation equation of the NGCG for an homogeneous and isotropic spacetime, this requires the function $\tilde{A}(a)$ to be of the form

$$\tilde{A}(a) = -w_X Aa^{-3(1+w_X)(1+\alpha)}, \quad (3)$$

where A is a positive constant, and the other positive constant B appears in Eq. (2) an integration constant. One can see explicitly that this model recovers the GCG model as the equation-of-state parameter w_X taken to be -1 , and an ordinary Λ CDM model can be reproduced by taking the parameter α to be zero. The parameter α is called *interaction parameter* of the model as will be shown below.

The NGCG scenario involves an interacting Λ CDM picture. For showing this, we first decompose the NGCG fluid into two components, one is the dark energy component, and the other is the dark matter component,

$$\rho_{\text{Ch}} = \rho_X + \rho_{dm}. \quad (4)$$

Note that the pressure of the NGCG fluid is provided only by the dark energy component, namely $p_{\text{Ch}} = p_X$. Therefore, the energy density of the dark energy ingredient can be given

$$\rho_X = \frac{p_{\text{Ch}}}{w_X} = \frac{Aa^{-3(1+w_X)(1+\alpha)}}{[Aa^{-3(1+w_X)(1+\alpha)} + Ba^{-3(1+\alpha)}]^{\frac{\alpha}{1+\alpha}}} , \quad (5)$$

and then the energy density of the dark matter component can also be obtained

$$\rho_{dm} = \frac{Ba^{-3(1+\alpha)}}{[Aa^{-3(1+w_X)(1+\alpha)} + Ba^{-3(1+\alpha)}]^{\frac{\alpha}{1+\alpha}}} . \quad (6)$$

From these expressions one obtains the scaling behavior of the energy densities

$$\frac{\rho_{dm}}{\rho_X} = \frac{B}{A} a^{3w_X(1+\alpha)} . \quad (7)$$

We see explicitly from it that there must exist an energy flow between dark matter and dark energy provided that $\alpha \neq 0$. When $\alpha > 0$, the transfer direction of the energy flow is from dark matter to dark energy; when $\alpha < 0$, just the reverse. Therefore, it is clear that the parameter α characterizes the interaction between dark energy and dark matter. This is the reason for that we call α the interaction parameter.

The parameters A and B can be expressed in terms of current cosmological observables. From Eq.(2), it is easy to get

$$A + B = \rho_{\text{Ch}0}^\eta , \quad (8)$$

where $\eta = 1 + \alpha$ is used to characterize the interaction for simplicity, thus we have

$$A = \rho_{\text{Ch}0}^\eta A_s , \quad B = \rho_{\text{Ch}0}^\eta (1 - A_s) , \quad (9)$$

where A_s is a dimensionless parameter. Using Eqs. (7) and (9), one gets

$$A_s = \frac{\rho_{X0}}{\rho_{X0} + \rho_{dm0}} = \frac{\Omega_X^0}{1 - \Omega_b^0} , \quad (10)$$

where the second equality stands for the cosmological model involving the baryon matter component. We have assumed here that the space of the Universe is flat. Hence, the NGCG energy density can be expressed as

$$\rho_{\text{Ch}} = \rho_{\text{Ch}0} a^{-3} [1 - A_s(1 - a^{-3w_X\eta})]^{1/\eta} . \quad (11)$$

Making use of Eqs. (2), (5), (6), and (11), the energy densities of dark energy and dark matter can be re-expressed as

$$\rho_X = \rho_{X0} a^{-3(1+w_X\eta)} \left[1 - \frac{\Omega_X^0}{1 - \Omega_b^0} (1 - a^{-3w_X\eta}) \right]^{\frac{1}{\eta}-1} , \quad (12)$$

$$\rho_{dm} = \rho_{dm0} a^{-3} \left[1 - \frac{\Omega_X^0}{1 - \Omega_b^0} (1 - a^{-3w_X\eta}) \right]^{\frac{1}{\eta}-1} . \quad (13)$$

The whole NGCG fluid satisfies the energy conservation, but dark energy and dark matter components do not obey the energy conservation separately; they interact with each other. We depict this interaction through an energy exchange term Q . The equations of motion for dark energy and dark matter can be written as

$$\dot{\rho}_X + 3H(1 + w_X)\rho_X = Q , \quad (14)$$

$$\dot{\rho}_{dm} + 3H\rho_{dm} = -Q , \quad (15)$$

where dot denotes a derivative with respect to time t , and $H = \dot{a}/a$ represents the Hubble parameter. For convenience we define the effective equations of state for dark energy and dark matter through the parameters

$$w_X^{(e)} = w_X - \frac{Q}{3H\rho_X} , \quad (16)$$

$$w_{dm}^{(e)} = \frac{Q}{3H\rho_{dm}} . \quad (17)$$

According to the definition of the effective equations of state, the equations of motion for dark energy and dark matter can be re-expressed into forms of energy conservation,

$$\dot{\rho}_X + 3H(1 + w_X^{(e)})\rho_X = 0 , \quad (18)$$

$$\dot{\rho}_{dm} + 3H(1 + w_{dm}^{(e)})\rho_{dm} = 0 . \quad (19)$$

By means of the concrete forms of dark energy and dark matter in NGCG scenario, Eqs. (12) and (13), one can obtain

$$w_X^{(e)} = w_X + \frac{(\eta - 1)w_X(1 - \Omega_X^0 - \Omega_b^0)a^{3w_X\eta}}{\Omega_X^0 + (1 - \Omega_X^0 - \Omega_b^0)a^{3w_X\eta}} , \quad (20)$$

$$w_{dm}^{(e)} = -\frac{(\eta - 1)w_X\Omega_X^0}{\Omega_X^0 + (1 - \Omega_X^0 - \Omega_b^0)a^{3w_X\eta}} . \quad (21)$$

Now we switch to discuss the cosmological evolution. Consider a spatially flat FRW Universe with baryon matter component ρ_b and NGCG fluid ρ_{Ch} , the Friedmann equation reads

$$3M_P^2 H^2 = \rho_{Ch} + \rho_b , \quad (22)$$

where M_P is the reduced Planck mass. The Friedmann equation can also be expressed as

$$H(a) = H_0 E(a) , \quad (23)$$

where

$$E(a) = \left\{ (1 - \Omega_b^0) a^{-3} \left[1 - \frac{\Omega_X^0}{1 - \Omega_b^0} (1 - a^{-3w_X \eta}) \right]^{1/\eta} + \Omega_b^0 a^{-3} \right\}^{1/2} . \quad (24)$$

Then, the fractional energy densities of various components can be easily obtained

$$\Omega_X = \Omega_X^0 E^{-2} a^{-3(1+w_X \eta)} \left[1 - \frac{\Omega_X^0}{1 - \Omega_b^0} (1 - a^{-3w_X \eta}) \right]^{\frac{1}{\eta} - 1} , \quad (25)$$

$$\Omega_{dm} = (1 - \Omega_X^0 - \Omega_b^0) E^{-2} a^{-3} \left[1 - \frac{\Omega_X^0}{1 - \Omega_b^0} (1 - a^{-3w_X \eta}) \right]^{\frac{1}{\eta} - 1} , \quad (26)$$

$$\Omega_b = \Omega_b^0 E^{-2} a^{-3} . \quad (27)$$

So far we see clearly that the NGCG model is totally dual to a coupled dark energy scenario [21,22], namely an interacting XCDM parametrization. It is remarkable that the interaction between dark energy and dark matter can be interpreted as arising from the time variation of the mass of dark matter particles. The GCG model is a special case in the NGCG model corresponding to $w_X = -1$, thus the GCG model is actually an interacting Λ CDM model. Fig.1 and Fig.2 illustrate examples of the density evolution in the NGCG model. The current density parameters used in the plots are $\Omega_{dm}^0 = 0.25$, $\Omega_X^0 = 0.7$, and $\Omega_b^0 = 0.05$. In Fig.1, we show the cases having the common equation-of-state parameter $w_X = -1.2$, while the interaction parameters α are taken to be 0, 0.5, and 0.8, respectively. Note that the $\alpha = 0$ case corresponds to a normal phantom model with constant w_X . In this example we see the role the interaction parameter α plays in the model. The transfer energy flows from dark matter to dark energy when $\alpha > 0$; the larger α leads to the stronger energy flow; density of baryon component is also affected evidently by the interaction between dark energy and dark matter. In Fig.2, we depict the cases with common interaction parameter $\alpha = 0.5$, and the equation-of-state parameters w_X are taken to be -1 , -0.8 , and -1.2 , respectively. Here $w_X = -1$ case corresponds exactly to the GCG model. The effect of the parameter w_X in the NGCG scenario is also evident as we see in this example.

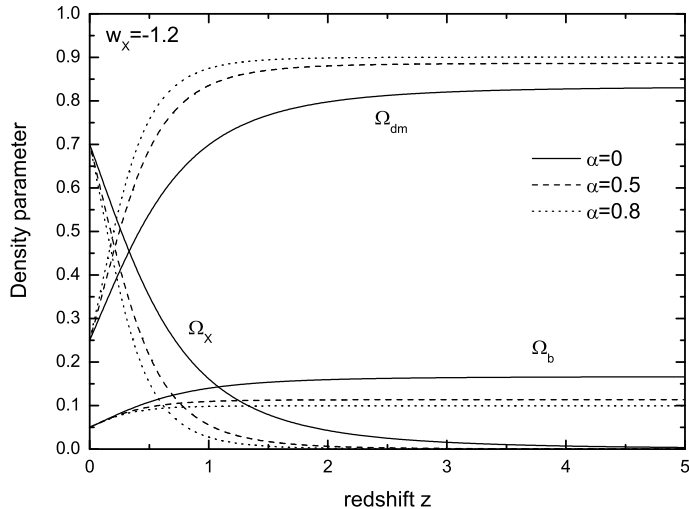


FIG. 1. The evolution of the density parameters for various components Ω_X , Ω_{dm} , and Ω_b . Note that $\Omega_{Ch} = \Omega_X + \Omega_{dm}$. The current density parameters used in the plot are $\Omega_{dm}^0 = 0.25$, $\Omega_X^0 = 0.7$, and $\Omega_b^0 = 0.05$. In this case, we fix w_X and vary α .

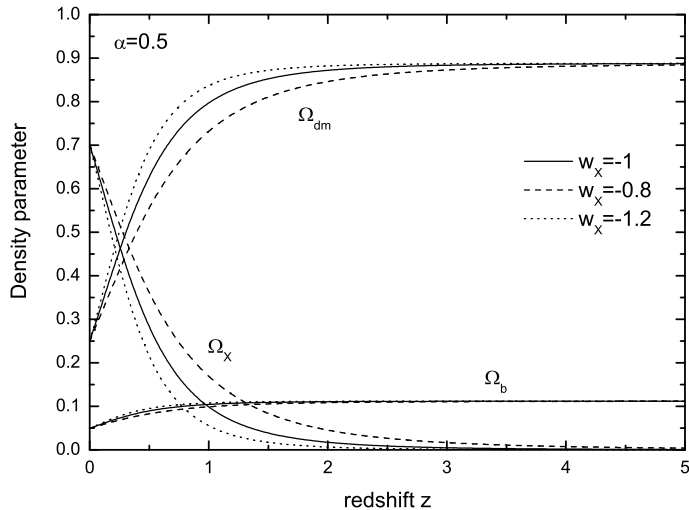


FIG. 2. The evolution of the density parameters for various components Ω_X , Ω_{dm} , and Ω_b . Note that $\Omega_{Ch} = \Omega_X + \Omega_{dm}$. The current density parameters used in the plot are $\Omega_{dm}^0 = 0.25$, $\Omega_X^0 = 0.7$, and $\Omega_b^0 = 0.05$. In this case, we fix α and vary w_X .

Let us now discuss the cosmological consequences led by the NGCG model and compare the cosmological quantities in the NGCG cosmology with those of some special cases such as Λ CDM and GCG. Firstly, we regard the Hubble parameter H which evaluates the velocity of the expansion of the Universe. In Fig.3 we plot the Hubble parameter of the NGCG model in units of $H_{\Lambda\text{CDM}}$ as a function of redshift z range from 0 to 5. The current density parameters used in the plot of Fig.3 are the same as used in Figs.1 and 2. The model parameters are

divided into two groups, $\alpha = 0$ and $\alpha = 0.5$, both including $w_X = -1, -0.8$, and -1.2 . It can be seen from Fig.3 that the NGCG model degenerates to the Λ CDM when the parameter α takes 0; the cases of $w_X > -1$ and $w_X < -1$ make H larger than and less than $H_{\Lambda\text{CDM}}$, respectively, during the cosmological evolution. The introducing of the interaction parameter α makes H be larger than $H_{\Lambda\text{CDM}}$ evidently at early times; while it is interesting to see that the value of $H/H_{\Lambda\text{CDM}}$ can cross 1 in the case of $w_X < -1$ in recent period. The acceleration of the Universe is evaluated by the deceleration parameter $q = -\ddot{a}/aH^2$. Omitting the radiation component, the deceleration parameter can be expressed as

$$q = \frac{1}{2} + \frac{3}{2}w_X\Omega_X, \quad (28)$$

where Ω_X is given by (25). The evolution of the deceleration parameter q is depicted in Fig.3 for selected parameter sets. The current density parameters are taken to be the same as above figures. The influence coming from the interaction α and equation of state of dark energy w_X can be seen clearly in this figure. We notice that a positive α makes the redshift of acceleration/deceleration transition ($q(z_T) = 0$) shift to a smaller value; while the values of z_T are nearly degenerate under the same α as shown in this example.

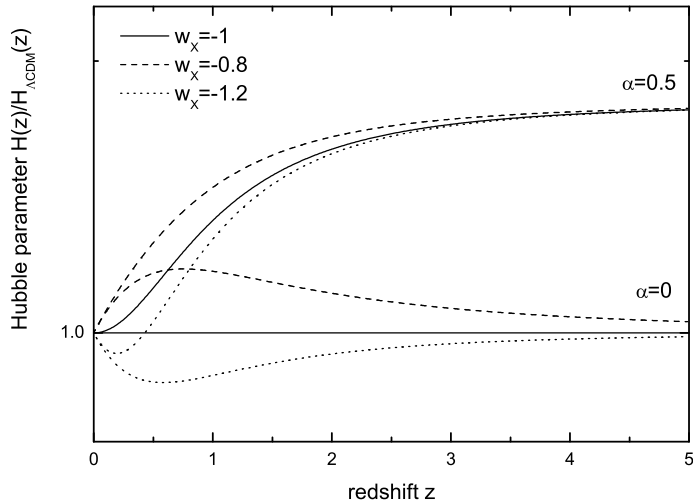


FIG. 3. The evolution of the Hubble parameter in units of $H_{\Lambda\text{CDM}}(z)$. The current density parameters are taken to be $\Omega_{dm}^0 = 0.25$, $\Omega_X^0 = 0.7$, and $\Omega_b^0 = 0.05$.

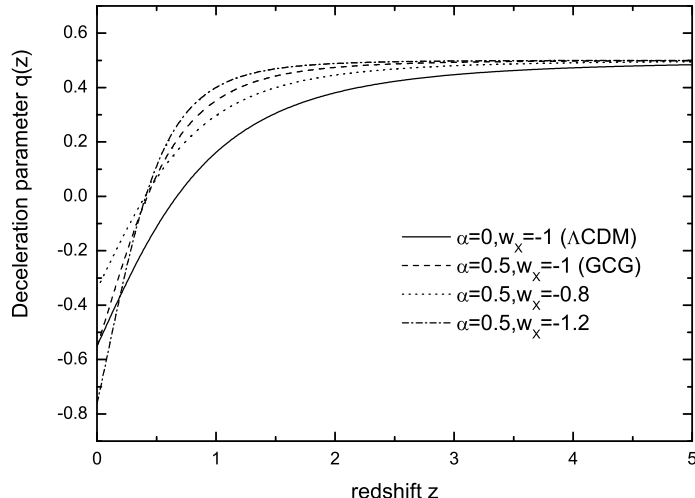


FIG. 4. The evolution of the deceleration parameter $q(z)$. The current density parameters are taken to be $\Omega_{dm}^0 = 0.25$, $\Omega_X^0 = 0.7$, and $\Omega_b^0 = 0.05$.

III. STATEFINDER DIAGNOSTIC

Since more and more dark energy models have been constructed for interpreting or describing the cosmic acceleration, the problem of discriminating between the various contenders becomes very important. In order to be able to differentiate between those competing cosmological scenarios involving dark energy, a sensitive and robust diagnostic for dark energy models is a must. For this purpose a diagnostic proposal that makes use of parameter pair $\{r, s\}$, the so-called “statefinder”, was introduced by Sahni et al. [23]. The statefinder probes the expansion dynamics of the Universe through higher derivatives of the scale factor \ddot{a} and is a natural companion to the deceleration parameter q which depends upon \ddot{a} . The statefinder pair $\{r, s\}$ is defined as follows

$$r \equiv \frac{\ddot{a}}{aH^3}, \quad s \equiv \frac{r - 1}{3(q - 1/2)}. \quad (29)$$

The statefinder is a “geometrical” diagnostic in the sense that it depends upon the scale factor and hence upon the metric describing space-time.

Trajectories in the $s - r$ plane corresponding to different cosmological models exhibit qualitatively different behaviors. The spatially flat Λ CDM scenario corresponds to a fixed point in the diagram

$$\{s, r\} \Big|_{\Lambda\text{CDM}} = \{0, 1\}. \quad (30)$$

Departure of a given dark energy model from this fixed point provides a good way of establishing the “distance” of this model from Λ CDM [23,24]. As demonstrated in Refs. [23–29]

the statefinder can successfully differentiate between a wide variety of dark energy models including the cosmological constant, quintessence, quintom, the Chaplygin gas, braneworld models, holographic dark energy and interacting dark energy models. We can clearly identify the “distance” from a given dark energy model to the Λ CDM scenario by using the $r(s)$ evolution diagram.

The current location of the parameters s and r in these diagrams can be calculated in models, and on the other hand it can also be extracted from data coming from SNAP (Supernovae Acceleration Probe) type experiments [23,24]. Therefore, the statefinder diagnostic combined with future SNAP observations may possibly be used to discriminate between different dark energy models. In this section we apply the statefinder diagnostic to the NGCG model.

In what follows we will calculate the statefinder parameters for the NGCG model and plot the evolution trajectories of the model in the statefinder parameter-plane. The statefinder parameters can be expressed in terms of the total energy density ρ and the total pressure p in the Universe:

$$r = 1 + \frac{9(\rho + p)}{2\rho} \frac{\dot{p}}{\dot{\rho}}, \quad s = \frac{(\rho + p)}{p} \frac{\dot{p}}{\dot{\rho}}. \quad (31)$$

The total energy of the Universe is conserved, so we have $\dot{\rho} = -3H(\rho + p)$. Since the dust matter does not have pressure, the total pressure of the cosmic fluids is provided only by dark energy component, $p = p_X = w_X \rho_X$. Then making use of $\dot{\rho} = -3H(\rho + p)$ and $\dot{\rho}_X = -3H(1 + w_X^{(e)})\rho_X$, we can get the concrete expression of the statefinder parameters

$$r = 1 + \frac{9}{2} w_X \Omega_X (1 + w_X^{(e)}), \quad s = 1 + w_X^{(e)}. \quad (32)$$

Here $w_X^{(e)}$ and Ω_X are given by (20) and (25), respectively. Though the relationship between statefinder parameters r and s , namely the function $r(s)$, might be derived analytically in principle, we do not give the expression here due to the complexity of the formula. Making the redshift $z = 1/a - 1$ vary in an enough large range involving far future and far past, e.g. from -1 to 5 , one can easily get the evolution trajectories in the statefinder $s - r$ plane of this model. Selected curves of $r(s)$ are plotted in Fig.5 and Fig.6. In Fig.5, we fix $\alpha = 0.5$ and vary w_X as -0.8 , -1 , and -1.2 , respectively. In Fig.6, we fix $w_X = -1.2$ and vary α as 0 , ± 0.2 , ± 0.5 , and ± 0.8 , respectively. Other parameters are taken as the same as previous figures. In these two figures, dots locate the today’s values of the statefinder parameters (s_0, r_0) and arrows denote the evolution directions of the statefinder trajectories $r(s)$. The Λ CDM model locates at $(0, 1)$ in the $s - r$ plane also denoted as a dot.

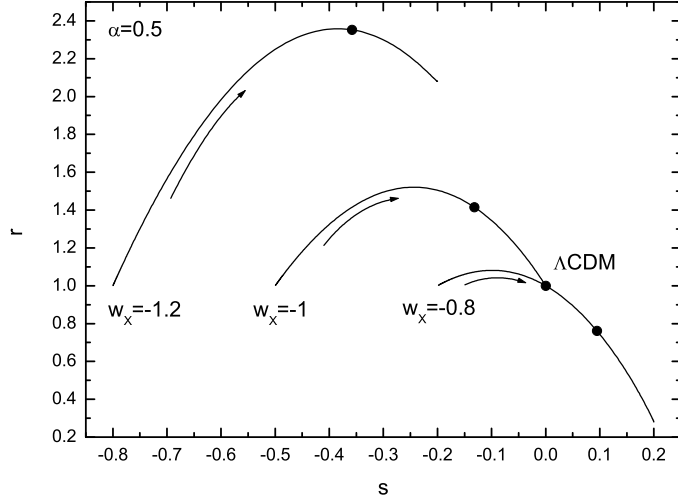


FIG. 5. The statefinder $r(s)$ evolution diagram. Dots locate the today's values of the statefinder parameters (s_0, r_0) and arrows denote the evolution directions of the statefinder trajectories $r(s)$. The Λ CDM model locates at the fixed point $(0, 1)$. In this case, we fix $\alpha = 0.5$ and vary w_X as -0.8 , -1 , and -1.2 , respectively.

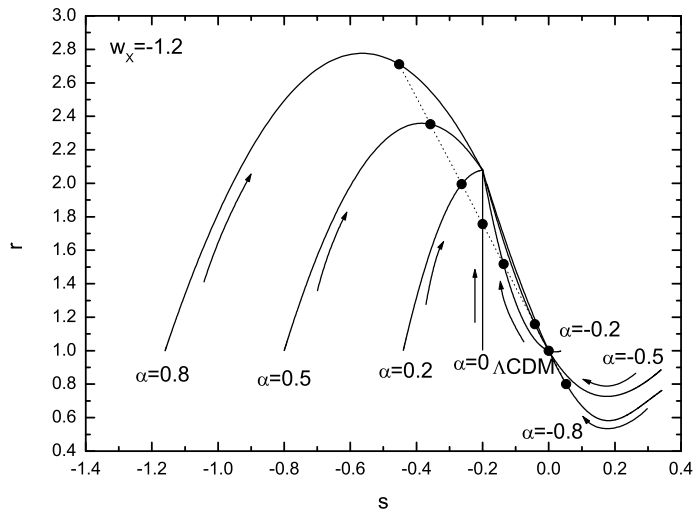


FIG. 6. The statefinder $r(s)$ evolution diagram. Dots locate the today's values of the statefinder parameters (s_0, r_0) and arrows denote the evolution directions of the statefinder trajectories $r(s)$. The Λ CDM model locates at the fixed point $(0, 1)$. In this case, we fix $w_X = -1.2$ and vary α as 0 , ± 0.2 , ± 0.5 , and ± 0.8 , respectively.

The statefinder diagnostic can discriminate between various dark energy models effectively. Different cosmological models involving dark energy exhibit qualitatively different evolution trajectories in the $s - r$ plane. For example, the Λ CDM scenario corresponds to the fixed point $s = 0$, $r = 1$ as shown in (30), and the SCDM (standard cold dark matter) scenario corresponds to the point $s = 1$, $r = 1$. For the “quiescence” (XCDM)

models, the trajectories are some vertical segments, i.e. r decreases monotonically from 1 to $1 + \frac{9}{2}w_X(1 + w_X)$ while s remains constant at $1 + w_X$ [23,24]. The quintessence (inverse power law) tracker models have typical trajectories similar to arcs of an upward parabola lying in the regions $s > 0$, $r < 1$ [23,24]. The holographic dark energy scenario ($c = 1$ case), as shown in [27], commences its evolution from $s = 2/3$, $r = 1$, through an arc segment, and ends it at the Λ CDM fixed point ($s = 0$, $r = 1$) in the future. The coupled quintessence models and Quintom models exhibit more complicated trajectories as shown in Refs. [25,29]. Now from the Figs. 5 and 6 of this paper, we can see the statefinder trajectories of the NGCG model. In Fig.5 we see the cases under the fixed α , where the GCG model ($w_X = -1$) exhibits a complete downward parabola, while the general cases ($w_X \neq -1$) correspond to some broken parabolas. The statefinder trajectory commences its evolution from $s = 1 + (1 + \alpha)w_X$, $r = 1$ at $t \rightarrow 0$ to $s = 1 + w_X$, $r = 1 + \frac{9}{2}w_X(1 + w_X)$ at $t \rightarrow \infty$, through the curve. Today's statefinder point locates at $s_0 = 1 + w_{X0}^{(e)}$, $r_0 = 1 + \frac{9}{2}w_X\Omega_X^0(1 + w_{X0}^{(e)})$, where $w_{X0}^{(e)} = w_X + \alpha w_X(1 - \Omega_X^0 - \Omega_b^0)/(1 - \Omega_b^0)$. The “distance” from the NGCG model to the Λ CDM scenario can be measured directly in the statefinder plane. Note that under a positive α , the cases of $w_X < -1$ never arrive at the Λ CDM fixed point; the GCG case ($w_X = -1$) ends at the Λ CDM fixed point; while the cases of $w_X > -1$ have passed through this fixed point. Fig.6 displays the cases under a fixed w_X . We show here $w_X = -1.2$, a phantom. Trajectories correspond to zero, positive, as well as negative values of α are all displayed in this diagram to depict a complete statefinder diagnostic. It is interesting to see that the trajectories can pass through the Λ CDM fixed point under a phantom case when $\alpha < 0$. This is because a negative α makes dark energy component transfer energy flow to dark matter component. We notice that the normal phantom case ($\alpha = 0$) evolves its trajectory along a vertical segment. Comparing with the quiescence case [23,24], the phantom case reposes on the left of Λ CDM point, namely the region $s < 0$, $r > 1$, and evolves upwards; while the quiescence case reposes on the right of the Λ CDM point, namely the region $s > 0$, $r < 1$, and evolves downwards. Interestingly, under a fixed w_X , the present statefinder points as well as the Λ CDM fixed point locate on a straight line. This is because when w_X is fixed, the relationship between r_0 and s_0 is linear, $r_0 = 1 + \frac{9}{2}w_X\Omega_X^0s_0$.

IV. OBSERVATIONAL CONSTRAINTS FROM SNE IA, CMB, AND LSS DATA

In this section we will derive the constraints on the NGCG model from current available observational data. It should be mentioned that the interacting XCDM parametrization scenario has been tested by the recent Type Ia supernovae data [21]. The results show that the SNe Ia data favor a negative coupling and an equation of state $w_X < -1$, namely a negatively coupled phantom dark energy. However, as we know, the supernovae data

alone are not sufficient to constrain dark energy models strictly (see e.g. the analysis in Ref. [14]). Therefore, to obtain more tight constraints on dark energy models, one should need additional data provided by other astronomical observations to be necessary and useful complements to the SNe data. It has been demonstrated that some observational quantities irrelevant to H_0 are very suitable to play this role [30]. Such quantities and data can be found in the probes of CMB and LSS [14,30,31]. In what follows we perform a combined analysis of SNe Ia, CMB, and LSS on the constraints of the NGCG model. We use a χ^2 statistic

$$\chi^2 = \chi_{\text{SN}}^2 + \chi_{\text{CMB}}^2 + \chi_{\text{LSS}}^2 , \quad (33)$$

where χ_{SN}^2 , χ_{CMB}^2 and χ_{LSS}^2 are contributions from SNe Ia, CMB, and LSS data, respectively. It is well known that the acceleration of the Universe is found by the Type Ia supernovae observations, where the concept of the luminosity distance plays a very important role. The luminosity distance of a light source is defined in such a way as to generalize to an expanding and curved space the inverse-square law of brightness valid in a static Euclidean space,

$$d_L = \left(\frac{\mathcal{L}}{4\pi\mathcal{F}} \right)^{1/2} = cH_0^{-1}(1+z) \int_0^z \frac{dz'}{E(z')} , \quad (34)$$

where \mathcal{L} is the absolute luminosity which is a known value for the standard candle SNe Ia, \mathcal{F} is the measured flux. The Hubble distance $cH_0^{-1} = 2997.9h^{-1}$ Mpc. The Type Ia supernova observations directly measure the apparent magnitude m of a supernova and its red-shift z . The apparent magnitude m is related to the luminosity distance d_L of the supernova through

$$m(z) = M + 5 \log_{10}(d_L(z)/\text{Mpc}) + 25 , \quad (35)$$

where M is the absolute magnitude which is believed to be constant for all Type Ia supernovae. In our analysis, we take the 157 gold data points listed in Riess et al. [16] which includes recent new 14 high redshift SNe (gold) data from the HST/GOODS program. The χ^2 function determined by SNe Ia observations is

$$\chi_{\text{SN}}^2 = \sum_{i=1}^{157} \frac{[\mu_{\text{obs}}(z_i) - \mu_{\text{th}}(z_i)]^2}{\sigma_i^2} , \quad (36)$$

where the extinction-corrected distance moduli $\mu(z)$ is defined as $\mu(z) = m(z) - M$, and σ_i is the total uncertainty in the observation. Following the Ref. [21], we fix $\Omega_b^0 = 0.05$ in the computation for simplification. Hence, the computation is carried out in a four-dimensional space, for the four parameters $P = (\eta, w_X, h, \Omega_{dm}^0)$. For the CMB, we use only the measurement of the CMB shift parameter [32],

$$\mathcal{R} = \sqrt{\Omega_m^0} \int_0^{z_{\text{dec}}} \frac{dz}{E(z)}, \quad (37)$$

where $\Omega_m^0 = \Omega_{dm}^0 + \Omega_b^0$, and $z_{\text{dec}} = 1089$ [2]. Note that this quantity is irrelevant to the parameter H_0 such that provides robust constraint on the dark energy model. The results from CMB data correspond to $\mathcal{R}_0 = 1.716 \pm 0.062$ (given by WMAP, CBI, ACBAR) [2,33]. We include the CMB data in our analysis by adding $\chi_{\text{CMB}}^2 = [(\mathcal{R} - \mathcal{R}_0)/\sigma_{\mathcal{R}}]^2$ (see [30]), where \mathcal{R} is computed by the NGCG model using equation (37). The only large scale structure information we use is the parameter A measured by SDSS [34], defined by

$$A = \sqrt{\Omega_m^0} E(z_1)^{-1/3} \left[\frac{1}{z_1} \int_0^{z_1} \frac{dz}{E(z)} \right]^{2/3}, \quad (38)$$

where $z_1 = 0.35$. Also, we find that this quantity is independent of H_0 either, thus can provide another robust constraint on the model. The SDSS gives the measurement data [34] $A_0 = 0.469 \pm 0.017$. We also include the LSS constraint in our analysis by adding $\chi_{\text{LSS}}^2 = [(A - A_0)/\sigma_A]^2$ (see [14,31]), where A is computed by the NGCG model using equation (38). Note that we have chosen to use only the most conservative and robust information, \mathcal{R} and A , from CMB and LSS observations. These measurements we use do not depend on the Hubble constant H_0 , thus are useful complementarities to the SNe data.

We now analyze the probability distribution of η and w_X in the NGCG model. The likelihood of these two parameters is determined by minimizing over the ‘‘nuisance’’ parameters

$$\mathcal{L}(\eta, w_X) = \int dh d\Omega_{dm}^0 e^{-\chi^2/2}, \quad (39)$$

where the integral is over a large enough range of h and Ω_{dm}^0 to include almost all the probability. We now compute $\mathcal{L}(\eta, w_X)$ on a two-dimensional grid spanned by η and w_X . The 68.3%, 95.4%, and 99.7% (namely 1, 2, and 3 σ) confidence contours consist of points where the likelihood equals $e^{-2.31/2}$, $e^{-6.18/2}$, and $e^{-11.83/2}$ of the maximum value of the likelihood, respectively. Fig.7 shows our main results, the contours of 1 σ , 2 σ , and 3 σ confidence levels in the $w_X - \eta$ plane. The 1 σ fit values for the model parameters are: $w_X = -0.98_{-0.20}^{+0.15}$ and $\eta = 1.06_{-0.16}^{+0.20}$, and the minimum value of χ^2 in the four dimensional parameter space is: $\chi_{\text{min}}^2 = 167.29$. We see clearly that the combined analysis of SNe Ia, CMB, and LSS data provides a fairly tight constraint on the NGCG model. It is remarkable that the best fit happens at the vicinity of the cosmological constant, even though w_X is slightly larger than -1 and η is mildly larger than 1 (i.e. α slightly larger than 0). This means that within the framework of the NGCG model the real form of dark energy at the maximum probability is the near cosmological constant according to the joint analysis of SNe+CMB+LSS data. However, the analysis results still accommodate the existence likelihood of the ‘‘X-matter’’ and the interaction between dark energy and dark matter. In 1 σ range, $w_X \in (-1.18, -0.83)$

and $\alpha \in (-0.1, 0.26)$. This implies that the probabilities of that dark energy behaves as quintessence-like form and phantom-like form are roughly equal, and the probabilities that the energy flow streams from dark energy to dark matter and the reverse are also roughly equal. One-dimensional likelihood distribution functions for w_X and η are shown in Fig.8 and Fig.9, respectively. It is very clear that the original Chaplygin gas model, $\alpha = 1$ (or $\eta = 2$) and $w_X = -1$, is totally ruled out by the observational data at 99.7% confidence level. In addition, it should be pointed out that when we fix $\eta = 2$ and let w_X free, the NGCG model will be identified as the so-called variable Chaplygin gas (VCG) model proposed in Ref. [35] (see also Ref. [36]). The joint analysis of SNe+CMB+LSS also rules out this probability. It is hopeful that the future precise data will provide more strong evidences to judge whether the dark energy is the cosmological constant and whether dark energy and dark matter are in unification.

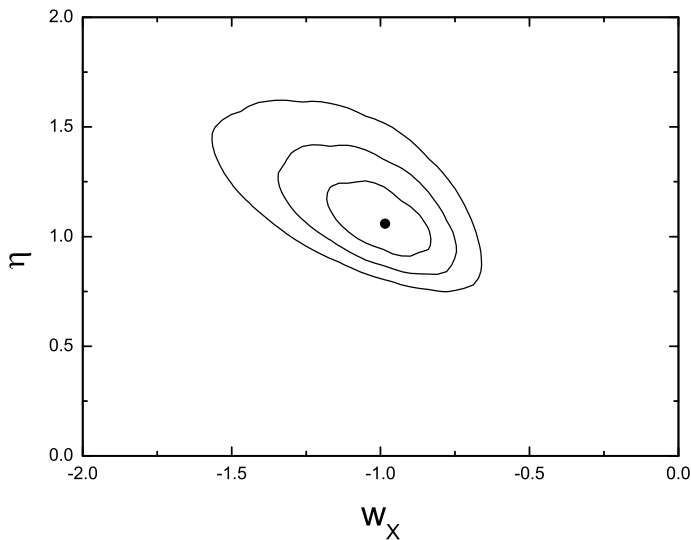


FIG. 7. Confidence level contours of 68.3%, 95.4% and 99.7% in the (w_X, η) plane. The 1σ fit values for the model parameters are: $w_X = -0.98^{+0.15}_{-0.20}$ and $\eta = 1.06^{+0.20}_{-0.16}$, and the minimum value of χ^2 in the four dimensional parameter space is: $\chi^2_{\min} = 167.29$.

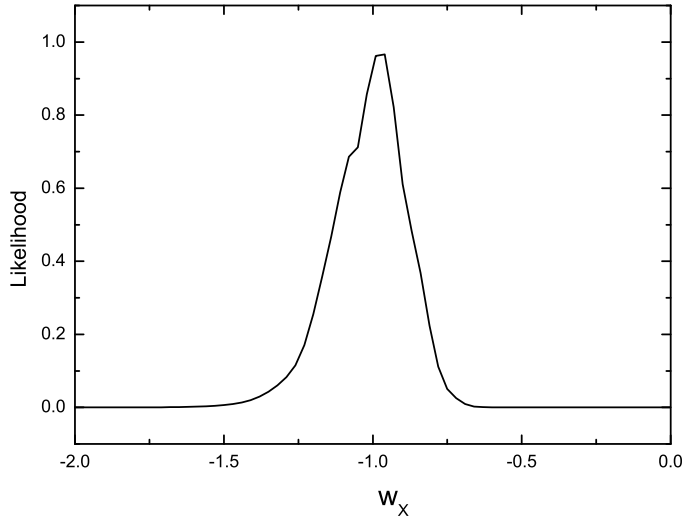


FIG. 8. One-dimensional probability distribution for w_X .

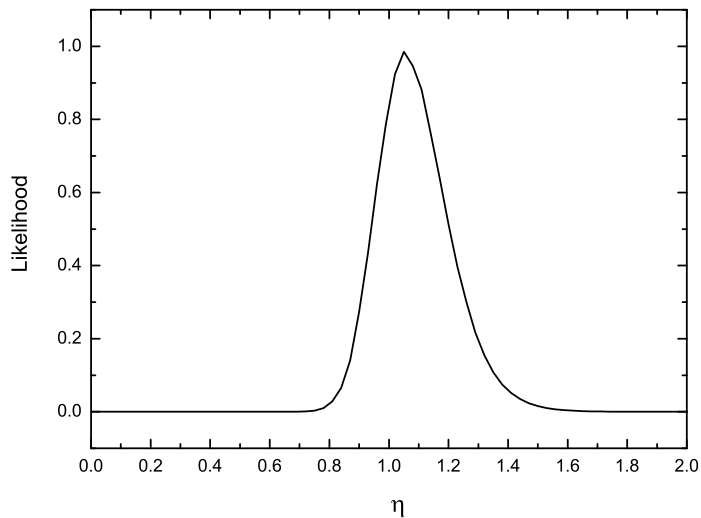


FIG. 9. One-dimensional probability distribution for η .

V. CONCLUDING REMARKS

The Chaplygin gas model is a proposal to describe dark energy and dark matter as a unified fluid, the Chaplygin gas, characterized by an exotic equation of state $p = -A/\rho$, where A is a positive constant. Since this original Chaplygin gas has been ruled out by the observations, by introducing a free parameter α , a generalization of the Chaplygin equation of state $p = -A/\rho^\alpha$ was considered. The generalized Chaplygin gas model is also regarded as a unification of dark energy and dark matter. The reason is that the GCG behaves as a

dust-like matter at early stage and as a cosmological constant at late stage. That is to say that the GCG model admits that the Universe will be dominated by a cosmological constant and thus enter into a de Sitter phase in the future. However, we can not hitherto affirm whether the dark energy is a tiny positive cosmological constant. Therefore, the scheme for unification of dark energy and dark matter should accommodate other forms of dark energy such as quintessence-like and phantom-like dark energy. This is the motivation for us to further generalize the GCG model.

We propose in this paper a new model as a scheme for the unification of dark energy and dark matter. This new model is a further extension version of the GCG model, thus dubbed new generalized Chaplygin gas model. This further generalization is implemented by introducing another free parameter w_X to make the constant A in the GCG equation of state become a scale factor dependent function $\tilde{A}(a)$. In order to implement the interpolation between a dust dominated Universe and an X-matter dominated Universe, the unique choice of $\tilde{A}(a)$ is $\tilde{A}(a) = -w_X A a^{-3(1+w_X)(1+\alpha)}$. Through a two-fluid decomposition, we show that the NGCG model is totally equivalent to an interacting XCDM parametrization scenario, in which the interaction between dark energy and dark matter is characterized by the constant α . We discuss the cosmological consequences led by such an unified dark sectors model. Furthermore, a statefinder diagnostic is performed on this scenario and the discrimination between this scenario and other dark energy models is shown. Finally, a combined analysis of the data of SNe Ia, CMB, and LSS is used to constrain the parameters of the NGCG model. The fit result shows that the joint analysis can provide a considerably tight constraint on the NGCG model. According to the observational test, the best fit happens at the vicinity of the Λ CDM. We hope that the future precise data will provide more strong evidences to judge whether the dark energy is the cosmological constant and whether dark energy and dark matter can be unified into one component. Also, it would be interesting to investigate the evolution of density perturbations and the structure formation in the NGCG scenario.

ACKNOWLEDGMENTS

One of us (X.Z.) is grateful to Xiao-Jun Bi, Zhe Chang, Zong-Kuan Guo, and Hao Wei for helpful discussions. This work was supported by the Natural Science Foundation of China (Grant No. 111105035001).

REFERENCES

- [1] A. G. Riess *et al.*, *Astron. J.* **116** (1998) 1009 [astro-ph/9805201]; S. Perlmutter *et al.*, *Astrophys. J.* **517** (1999) 565 [astro-ph/9812133].
- [2] C. L. Bennett *et al.*, *Astrophys. J. Suppl.* **148** (2003) 1 [astro-ph/0302207]; D. N. Spergel *et al.*, *Astrophys. J. Suppl.* **148** (2003) 175 [astro-ph/0302209].
- [3] M. Tegmark *et al.*, *Phys. Rev. D* **69** (2004) 103501 [astro-ph/0310723]; M. Tegmark *et al.*, *Astrophys. J.* **606** (2004) 702 [astro-ph/0310725].
- [4] S. Weinberg, *Rev. Mod. Phys.* **61** (1989) 1; S. M. Carroll, *Living Rev. Rel.* **4** (2001) 1 [astro-ph/0004075]; P. J. E. Peebles and B. Ratra, *Rev. Mod. Phys.* **75** (2003) 559 [astro-ph/0207347]; T. Padmanabhan, *Phys. Rept.* **380** (2003) 235 [hep-th/0212290].
- [5] C. Wetterich, *Nucl. Phys. B* **302** (1988) 668; P. J. E. Peebles and B. Ratra, *Astrophys. J.* **325** (1988) L17; R. R. Caldwell, R. Dave and P. J. Steinhardt, *Phys. Rev. Lett.* **80** (1998) 1582 [astro-ph/9708069]; I. Zlatev, L. Wang and P. J. Steinhardt, *Phys. Rev. Lett.* **82** (1999) 896 [astro-ph/9807002]; P. J. Steinhardt, L. Wang and I. Zlatev, *Phys. Rev. D* **59** (1999) 123504 [astro-ph/9812313].
- [6] L. Amendola, *Phys. Rev. D* **62** (2000) 043511 [astro-ph/9908023]; L. Amendola, D. Tocchini-Valentini, *Phys. Rev. D* **64** (2001) 043509 [astro-ph/0011243]; L. Amendola, D. Tocchini-Valentini, *Phys. Rev. D* **66** (2002) 043528 [astro-ph/0111535]; L. Amendola, *Mon. Not. Roy. Astron. Soc.* **342** (2003) 221 [astro-ph/0209494]; M. Pietroni, *Phys. Rev. D* **67** (2003) 103523 [hep-ph/0203085]; D. Comelli, M. Pietroni, and A. Riotto, *Phys. Lett. B* **571** (2003) 115 [hep-ph/0302080]; U. Franca, and R. Rosenfeld, *Phys. Rev. D* **69** (2004) 063517 [astro-ph/0308149]; X. Zhang, *Mod. Phys. Lett. A* **20** (2005) 2575 [astro-ph/0503072].
- [7] T. Chiba, T. Okabe and M. Yamaguchi, *Phys. Rev. D* **62** (2000) 023511 [astro-ph/9912463]; C. Armendariz-Picon, V. Mukhanov and P. J. Steinhardt, *Phys. Rev. Lett.* **85** (2000) 4438 [astro-ph/0004134]. C. Armendariz-Picon, V. Mukhanov and P. J. Steinhardt, *Phys. Rev. D* **63** (2001) 103510 [astro-ph/0006373]; T. Chiba, *Phys. Rev. D* **66** (2002) 063514 [astro-ph/0206298].
- [8] V. Sahni and A. Starobinsky, *Int. J. Mod. Phys. D* **9** (2000) 373 [astro-ph/9904398]; V. Sahni, *Class. Quant. Grav.* **19** (2002) 3435 [astro-ph/0202076]; L. A. Urena-Lopez and T. Matos, *Phys. Rev. D* **62** (2000) 081302 [astro-ph/0003364].
- [9] L. Randall and R. Sundrum, *Phys. Rev. Lett.* **83** (1999) 4690- [hep-th/9906064]; T. Shiromizu, K. Maeda, and M. Sasaki, *Phys. Rev. D* **62** (2000) 024012 [gr-qc/9910076]; R. Maartens, D. Wands, B. Bassett, and I. Heard, *Phys. Rev. D* **62** (2000) 041301 [hep-ph/9912464]; C. Deffayet, G. Dvali, and G. Gabadadze, *Phys. Rev. D* **65** (2002) 044023 [astro-ph/0105068]; C. Deffayet, S. J. Landau, J. Raux, M. Zaldarriaga, and P. Astier,

- Phys. Rev. D **66** (2002) 024019 [astro-ph/0201164]; V. Sahni and Y. Shtanov, JCAP **0311** (2003) 014 [astro-ph/0202346]; H. Collins and B. Holdom, Phys. Rev. D **62** (2000) 105009 [hep-ph/0003173]; R. Maartens, Living Rev. Rel. **7** (2004) 7 [gr-qc/0312059].
- [10] G. W. Gibbons, Phys. Lett. B **537** (2002) 1 [hep-th/0204008]; M. Fairbairn and M. H. G. Tytgat, Phys. Lett. B **546** (2002) 1 [hep-th/0204070]; S. Mukohyama, Phys. Rev. D **66** [hep-th/0204084]; (2002) 024009 A. Frolov, L. Kofman, and A. Starobinsky, Phys. Lett. B **545** (2002) 8 [hep-th/0204187]; Y.-S. Piao, R.-G. Cai, X. Zhang, and Y.-Z. Zhang, Phys. Rev. D **66** (2002) 121301 [hep-ph/0207143]; T. Padmanabhan and T. R. Choudhury, Phys. Rev. D **66** (2002) 081301 [hep-th/0205055]; T. Padmanabhan, Phys. Rev. D **66** (2002) 021301 [hep-th/0204150].
- [11] A. Y. Kamenshchik, U. Moschella, and V. Pasquier, Phys. Lett. B **511** (2001) 265 [gr-qc/0103004]; N. Bilic, G. B. Tupper, and R. D. Viollier, Phys. Lett. B **535** (2002) 17 [astro-ph/0111325]; M. C. Bento, O. Bertolami, and A. A. Sen, Phys. Rev. D **66** (2002) 043507 [gr-qc/0202064].
- [12] M. C. Bento, O. Bertolami, and A. A. Sen, Phys. Rev. D **67** (2003) 063003 [astro-ph/0210468]; M. C. Bento, O. Bertolami, and A. A. Sen, Phys. Rev. D **70** (2004) 083519 [astro-ph/0407239]; M. C. Bento, O. Bertolami, and A. A. Sen, Phys. Lett. B **575** (2003) 172 [astro-ph/0303538]; O. Bertolami, A. A. Sen, S. Sen, and P. T. Silva, Mon. Not. Roy. Astron. Soc. **353** (2004) 329 [astro-ph/0402387]; M. C. Bento, O. Bertolami, N. M. C. Santos, and A. A. Sen, Phys. Rev. D **71** (2005) 063501 [astro-ph/0412638]; J. S. Alcaniz, D. Jain, and A. Dev, Phys. Rev. D **67** (2003) 043514 [astro-ph/0210476].
- [13] M. Li, Phys. Lett. B **603** (2004) 1 [hep-th/0403127]; K. Ke and M. Li, Phys. Lett. B **606** (2005) 173 [hep-th/0407056]; Y. Gong, Phys. Rev. D **70** (2004) 064029 [hep-th/0404030]; Y. S. Myung, Phys. Lett. B **610** (2005) 18 [hep-th/0412224]; Q. G. Huang and M. Li, JCAP **0408** (2004) 013 [astro-ph/0404229]; Q. G. Huang and M. Li, JCAP **0503** (2005) 001 [hep-th/0410095]; Q. G. Huang and Y. Gong, JCAP **0408** (2004) 006 [astro-ph/0403590]; Y. Gong, B. Wang and Y. Z. Zhang, Phys. Rev. D **72** (2005) 043510 [hep-th/0412218]; Z. Chang, F.-Q. Wu, and X. Zhang, astro-ph/0509531.
- [14] X. Zhang and F.-Q. Wu, Phys. Rev. D **72** (2005) 043524 [astro-ph/0506310].
- [15] R. A. Knop et al., Astrophys. J. **598** (2003) 102 [astro-ph/0309368].
- [16] A. G. Riess et al., Astrophys. J. **607** (2004) 665 [astro-ph/0402512].
- [17] R. R. Caldwell, Phys. Lett. B **545** (2002) 23 [astro-ph/9908168].
- [18] R. R. Caldwell, M. Kamionkowski, and N. N. Weinberg, Phys. Rev. Lett. **91** (2003) 071301 [astro-ph/0302506].
- [19] N. Bilic, G. B. Tupper, and R. D. Viollier, astro-ph/0207423.
- [20] R. Jackiw, "A Particle Field Theorist's Lectures on Supersymmetric, Non-Abelian Fluid

- Mechanics and d-Branes”, physics/0010042.
- [21] E. Majerotto, D. Sapone, and L. Amendola, astro-ph/0410543.
 - [22] R.-G. Cai and A. Wang, JCAP **0503** (2005) 002 [hep-th/0411025].
 - [23] V. Sahni, T. D. Saini, A. A. Starobinsky and U. Alam, JETP Lett. **77** (2003) 201 [astro-ph/0201498].
 - [24] U. Alam, V. Sahni, T. D. Saini and A. A. Starobinsky, Mon. Not. Roy. ast. Soc. **344** (2003) 1057 [astro-ph/0303009].
 - [25] P. Wu and H. Yu, gr-qc/0509036.
 - [26] V. Gorini, A. Kamenshchik and U. Moschella, Phys. Rev. D **67** (2003) 063509 [astro-ph/0209395].
 - [27] X. Zhang, Int. J. Mod. Phys. D **14** (2005) 1597 [astro-ph/0504586].
 - [28] W. Zimdahl and D. Pavon, Gen. Rel. Grav. **36** (2004) 1483 [gr-qc/0311067].
 - [29] X. Zhang, Phys. Lett. B **611** (2005) 1 [astro-ph/0503075].
 - [30] Y. Wang, and P. Mukherjee, Astrophys. J. **606** (2004) 654 [astro-ph/0312192]; Y. Wang, and M. Tegmark, Phys. Rev. Lett. **92** (2004) 241302 [astro-ph/0403292].
 - [31] Y. Gong, and Y.-Z. Zhang, Phys. Rev. D **72** (2005) 043518 [astro-ph/0502262].
 - [32] J. R. Bond, G. Efstathiou, and M. Tegmark, Mon. Not. Roy. Astron. Soc. **291** (1997) L33 [astro-ph/9702100]; A. Melchiorri, L. Mersini, C. J. Odman, and M. Trodden, Phys. Rev. D **68** (2003) 043509 [astro-ph/0211522]; C. J. Odman, A. Melchiorri, M. P. Hobson, and A. N. Lasenby, Phys. Rev. D **67** (2003) 083511 [astro-ph/0207286].
 - [33] CBI Collaboration, T. J. Pearson et al., Astrophys. J. **591** (2003) 556 [astro-ph/0205388]; ACBAR Collaboration, C. L. Kuo et al., Astrophys. J. **600** (2004) 32 [astro-ph/0212289].
 - [34] D. J. Eisenstein et al., astro-ph/0501171.
 - [35] Z.-K. Guo and Y.-Z. Zhang, astro-ph/0506091.
 - [36] Z.-K. Guo and Y.-Z. Zhang, astro-ph/0509790.